

# Suppressed Current Collapse in High Pressure Water Vapor Annealed AlGa<sub>0.2</sub>Ga<sub>0.8</sub>N/GaN HEMTs

Yohei Kobayashi<sup>1</sup>, Joel T. Asubar<sup>1,\*</sup>, Koji Yoshitsugu<sup>2</sup>, Hirokuni Tokuda<sup>1</sup>, Masahiro Horita<sup>2</sup>, Yukiharu Uraoka<sup>2</sup>, and Masaaki Kuzuhara<sup>1</sup>

<sup>1</sup>University of Fukui, <sup>2</sup>Nara Institute of Science and Technology  
\*e-mail: joel@u-fukui.ac.jp, Phone: +81-776-27-9925

**Keywords:** AlGa<sub>0.2</sub>Ga<sub>0.8</sub>N high-electron-mobility transistor (HEMT), on-resistance ( $R_{on}$ ), current collapse, normalized dynamic  $R_{on}$  (NDR), high pressure water vapor annealing (HPWVA)

## Abstract

We report on the effect of high pressure water vapor annealing (HPWVA) on the current collapse characteristics of AlGa<sub>0.2</sub>Ga<sub>0.8</sub>N high-electron-mobility transistors (HEMTs). It was found out that, compared with a control device, HPWVA-processed devices exhibited significantly reduced dynamic on-resistance ( $R_{on}$ ) during pulsed I-V measurements, indicating current collapse mitigation by HPWVA. X-ray photoelectron spectroscopy (XPS) results suggest oxygen incorporation which can eventually lead to the occupation of near-surface nitrogen vacancies and to the formation of an oxide layer suitable for passivation, both of which can bring about current collapse reduction. On the basis of this account, we believe that HPWVA is a promising alternative for achieving improved performance in AlGa<sub>0.2</sub>Ga<sub>0.8</sub>N HEMTs.

## INTRODUCTION

AlGa<sub>0.2</sub>Ga<sub>0.8</sub>N high-electron-mobility transistors (HEMTs) are among the leading candidate devices for high power, high temperature and high frequency applications because of the excellent intrinsic properties of GaN [1]. However, in spite of rapid advances in AlGa<sub>0.2</sub>Ga<sub>0.8</sub>N HEMT technology, the widespread implementation of these devices is still hampered by problematic issues particularly by the well-known current collapse. Current collapse, which is widely believed to be due to trapping of electrons on the AlGa<sub>0.2</sub>Ga<sub>0.8</sub>N surface [2], is manifested as a significant increase in on-resistance ( $R_{on}$ ) after switching the device from on to off state. Approaches in dealing with current collapse include subjecting the device to surface treatment prior to passivation. There have been reports that pre-passivation surface treatment of O<sub>2</sub> plasma [3-4] can enhance the performance of AlGa<sub>0.2</sub>Ga<sub>0.8</sub>N HEMTs. Meanwhile, previous works by Yoshitsugu and co-workers [5] have demonstrated the effectiveness of high pressure water vapor annealing (HPWVA) in improving the quality of Al<sub>2</sub>O<sub>3</sub> gate dielectric in n-GaN MOS capacitors. In this work, we demonstrate remarkable reduction of current collapse in AlGa<sub>0.2</sub>Ga<sub>0.8</sub>N HEMTs subjected to HPWVA prior to SiN passivation.

## DEVICE STRUCTURE AND FABRICATION

An Al<sub>0.2</sub>Ga<sub>0.8</sub>N/GaN heterostructure grown on a 4H-SiC substrate by metal organic chemical vapor deposition (MOCVD) technique was used as the starting wafer in the present study. The thickness of the AlGa<sub>0.2</sub>Ga<sub>0.8</sub>N barrier layer is 25 nm. Typical values of 2DEG sheet carrier density and mobility are  $1.0 \times 10^{13} \text{ cm}^{-2}$  and  $1500 \text{ cm}^2/(\text{V}\cdot\text{s})$ , respectively. The device fabrication process started with the formation of device mesa isolation by inductively coupled plasma reactive ion etching (ICP-RIE) using a gas mixture of BCl<sub>3</sub>/Cl<sub>2</sub>. After the dry etching process, a Ti/Al/Mo/Au multilayer was deposited and annealed at 850 °C for 30 s under N<sub>2</sub> atmosphere to form source and drain ohmic electrodes. Nominal contact and sheet resistance values of 0.4 Ω-mm and 550 Ω/sq, respectively, were obtained from transfer length method (TLM) test structures fabricated on the same wafer. A Ni/Au bilayer was then deposited to form Schottky gates. Prior to SiN passivation, the devices were subjected to HPWVA, illustrated in Fig. 1, under a constant pressure of 0.5 MPa and different annealing temperatures of 200 °C, 300 °C, and 400 °C for 30 minutes.

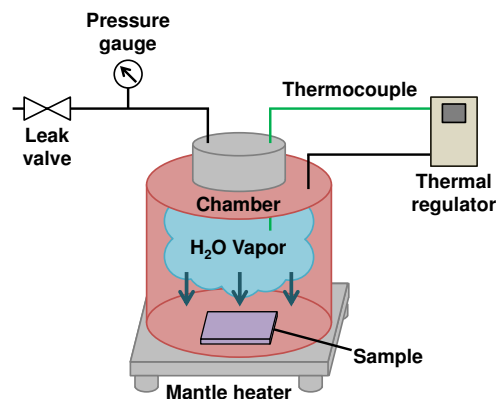


Fig. 1 Schematic illustration of high pressure water vapor annealing (HPWVA) experimental set-up.

For comparison, we also prepared a control device which was not subjected to the HPWVA process step. The un-annealed and high pressure water vapor-annealed devices, hereafter, will be referred to as reference and HPWV-annealed devices, respectively. A schematic illustration of a fabricated device, giving all the relevant dimensions, is given in Fig. 2. The gate length, gate width, gate-to-source spacing, and gate-to-drain spacing were 3  $\mu\text{m}$ , 100  $\mu\text{m}$ , 3  $\mu\text{m}$ , and 10  $\mu\text{m}$ , respectively.

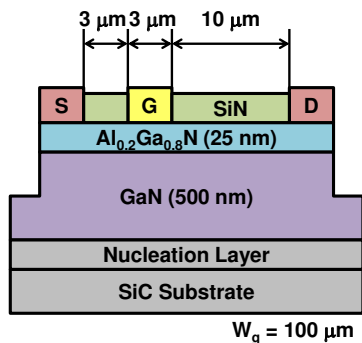


Fig. 2 Schematic cross-sectional illustration of AlGaIn/GaN HEMT used in this study.

## RESULTS AND DISCUSSION

Before carrying out current collapse measurements, we investigated if HPWVA has any detrimental effect on the device DC characteristics. The reference and HPWV-annealed devices exhibited essentially identical DC characteristics with nearly equal threshold voltage ( $V_{TH}$ ) of  $-3.1$  V and  $-3.0$  V, and with almost equal maximum drain current density of 480 mA/mm and 470 mA/mm at a gate-to-source voltage ( $V_{gs}$ ) of +1 V, respectively. We, therefore, concluded that HPWVA does not lead to any significant change in the device DC operation.

Figure 3 illustrates the current collapse evaluation performed on the devices. As shown in Fig. 3(a), a drain bias voltage of  $V_{DD} = 100$  V was used with a load resistance ( $R_L$ ) chosen to be approximately 10 k $\Omega$  so that the load line intersects the  $I_d$ - $V_{ds}$  curve below  $1/4$  of the maximum drain current. This ensured that  $R_{on}$  was reasonably measured in the linear region. To imitate a typical operation under which devices in power switching circuits are subjected, a train of gate pulses  $V_{gs}$  alternating between  $-5$  V (off-state) and +1 V (on-state) was applied to the gate terminal as shown in Fig. 3(b). After exactly pulse on-time ( $t_{on}$ ), the corresponding  $V_{ds}(t_{on})$  and  $I_{ds}(t_{on})$  were recorded, and the dynamic  $R_{on}$ , illustrated in Fig. 3(c), was calculated. For this particular experiment,  $t_{on}$  was varied from 1  $\mu\text{s}$  to 10 s while off-time ( $t_{off}$ ) was held constant at 100 ms.

As a method of representing current collapse quantitatively, we have introduced the normalized dynamic  $R_{on}$  (NDR) [6], which we have defined as the ratio of the dynamic  $R_{on}$  to static  $R_{on}$ . A higher NDR value indicates a higher degree of current collapse.

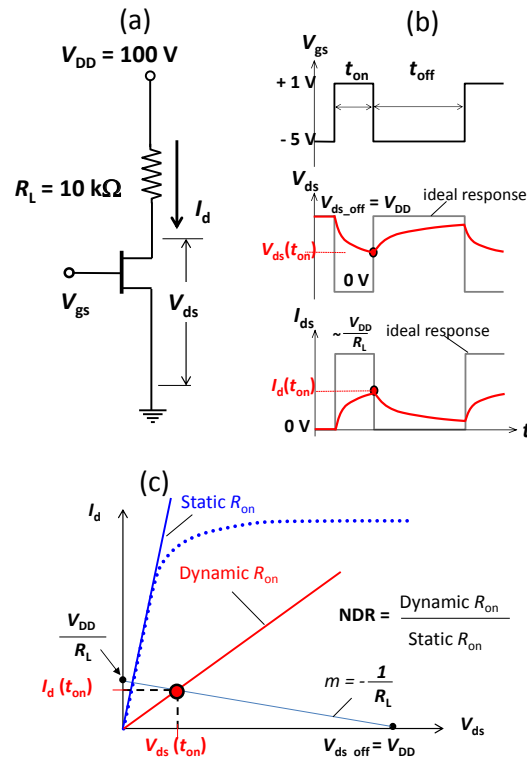


Fig. 3 Schematic illustration of (a) electrical circuit used in current collapse evaluation, (b) current and voltage waveforms, (c) load-line and dynamic  $R_{on}$  graphical definition.

The resulting dependence of NDR on  $t_{on}$  for all the devices under study is shown in Fig. 4. The trend of decreasing NDR with increasing  $t_{on}$  was expected for all devices because a longer  $t_{on}$  allows more time for detrapping of electrons, resulting in the greater recovery of  $R_{on}$ .

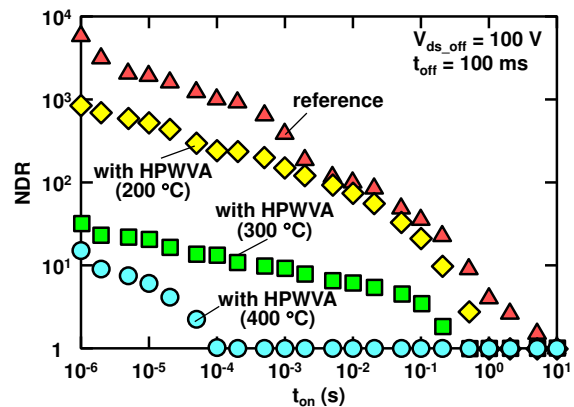


Fig. 4 Normalized dynamic  $R_{on}$  (NDR) dependence on on-time  $t_{on}$  of reference and HPWV-annealed devices.

Interestingly, however, compared with the reference device, all the HPWV-annealed devices exhibited lower NDR which was decreased with increasing annealing temperature used in this study. This result suggests the effectiveness of HPWVA in alleviating current collapse in AlGaIn/GaN HEMTs.

Following ref. [7], NDR can be expressed as a sum of pure exponential terms in the form:

$$NDR = 1 + \sum_{i=1}^n \alpha_i \exp\left(-\frac{t}{\tau_i}\right) \quad (1)$$

Here,  $\alpha_i$  represents the magnitude of the trapping process with time constant  $\tau_i$ . Fitting the experimentally measured NDR with the above relationship, we were able to obtain for the reference and HPWV-annealed (400 °C) devices the best fit curves (solid curves) and the corresponding exponential terms (dashed curves) given in Fig. 5.

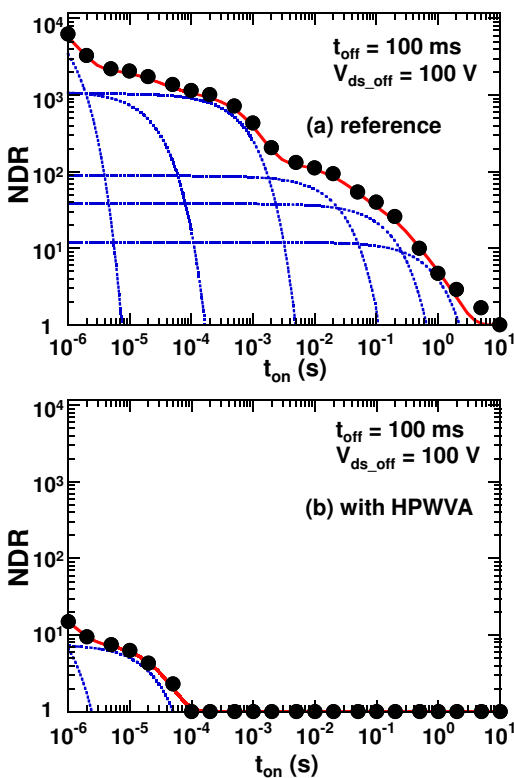


Fig. 5 Measured (solid data points) and calculated (solid curves) normalized dynamic  $R_{on}$  (NDR) dependence on  $t_{on}$  of (a) reference and (b) HPWV-annealed at 400 °C devices. Dashed curves represent extracted exponential terms.

Knowing the individual  $\tau_i$  of each exponential term, the corresponding  $(E_C - E_t)$  energy value can be obtained using the Shockley-Read-Hall (SRH) statistics [8]. Assuming an electron thermal velocity of  $2.6 \times 10^7$  cm/s, a capture cross-section of  $1.0 \times 10^{-15}$  cm<sup>2</sup>, and a density of states at conduction

band edge of  $2.2 \times 10^{18}$  cm<sup>-3</sup>, we obtained the  $(E_C - E_t)$  values summarized in Table I.

TABLE I  
Summary of extracted trap energy levels  $(E_C - E_t)$  for the reference and HPWV-annealed at 400 °C devices.

Device	$\tau_i$ (s)	$\alpha_i$	$E_C - E_t$ (eV)
reference	$8.0 \times 10^{-7}$	$1.2 \times 10^4$	0.28
	$2.4 \times 10^{-5}$	$1.1 \times 10^3$	0.37
	$7.1 \times 10^{-4}$	$1.0 \times 10^3$	0.45
	$2.5 \times 10^{-2}$	88	0.54
	$1.8 \times 10^{-1}$	38	0.59
	$9.0 \times 10^{-1}$	12	0.64
with HPWVA (400 °C)	$7.4 \times 10^{-7}$	25.9	0.28
	$2.5 \times 10^{-5}$	7.5	0.37

As can be seen from Fig. 5 and Table I, six trap levels, ranging from 0.28 to 0.6 eV, were obtained from the reference device. However, after HPWVA at 400 °C, only two shallow traps were detected at 0.28 and 0.37 eV. Moreover, the corresponding  $\alpha_i$  of these traps are orders of magnitude lower than those of the reference device. These results indicate the disappearance or weakening of all the other deeper traps after the HPWVA process. As these traps are likely to be connected to current collapse, the obtained data can explain the effective suppression of current collapse in HPWV-annealed devices.

In order to shed light on the effect of HPWVA on the AlGaIn surface from the chemical perspective, we performed X-ray photoelectron spectroscopy (XPS) analyses using a monochromatic Al K $\alpha$  radiation source ( $h\nu = 1486.6$  eV) on two separate AlGaIn surfaces, one was subjected to HPWVA at 400 °C (HPWV-annealed) and the other was untreated (reference). The O 1s core level spectra of the HPWV-annealed and reference samples taken with a photoelectron escape angle of 45° [9], which corresponds to a probing depth of 2–3 nm, are shown in Fig. 6.

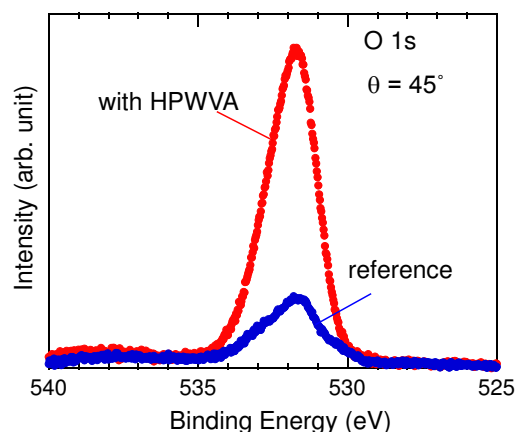


Fig. 6 O 1s XPS spectra of reference and HPWV-annealed (with HPWVA at 400 °C) samples taken at escape angle  $\theta = 45^\circ$ .

Note that the XPS profiles were calibrated to the adventitious C 1s peak position [10] and then normalized to their respective N 1s peak intensities. In comparison with the reference sample, the HPWV-annealed sample exhibited much higher O 1s peak intensity, suggesting oxygen incorporation and subsequent oxidation of the AlGaIn surface. It is also highly likely that some incorporated oxygen atoms fill up the near-surface nitrogen vacancies, which are believed to be partially, if not mainly, responsible for current collapse [11].

The oxidation of the surface after HPWVA was also confirmed by the Ga 3d spectra from both reference and HPWV-annealed surfaces. As shown in Fig. 7, the Ga 3d XPS signal of the HPWV-annealed sample is shifted towards the higher binding energy direction relative to that of the reference sample.

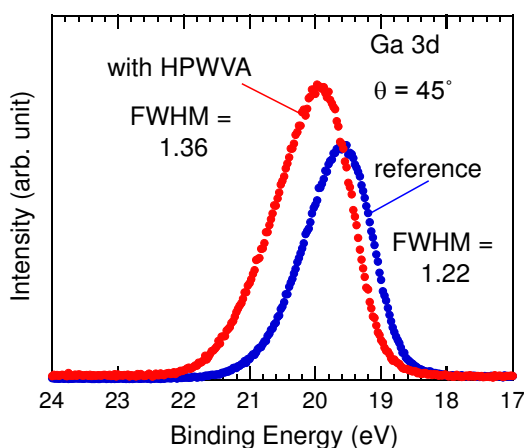


Fig. 7 Ga 3d XPS spectra of reference and HPWV-annealed (with HPWVA at 400 °C) samples taken at escape angle  $\theta = 45^\circ$ .

In addition, the full width at half maximum (FWHM) of HPWV-annealed sample Ga 3d peak is evidently broader. Both these results indicate the formation of surface oxide layer [12]. We believe that, aside from well-known Ga<sub>2</sub>O<sub>3</sub>, it is plausible that Ga<sub>2</sub>O sub-oxide is also formed on the HPWV-annealed surface via the chemical reaction:  $\text{Ga}_2\text{O}_3 + 4\text{H} \leftrightarrow \text{Ga}_2\text{O} + 2\text{H}_2\text{O}$  [13–14], which is made possible by the presence of hydrogen atom species from the high pressure water vapor [15]. In fact, initial deconvolution of the Ga 3d XPS spectra (not shown) suggests the presence of Ga<sub>2</sub>O sub-oxide in the HPWV-annealed sample. Previous reports indicate that Ga<sub>2</sub>O interfacial passivation layers may be essential for a low defect density of III-V surfaces [16–18]. Hinkle et al. have reported detection of a stable Ga<sub>2</sub>O interfacial layer and its favorable impact on passivation [19]. However, because of the degree of complexity involved [20], a more thorough investigation is necessary to support the Ga<sub>2</sub>O sub-oxide formation hypothesis. Nonetheless, we believe that the HPWVA process promotes the formation of an oxide layer highly suitable for stable device passivation.

## CONCLUSIONS

We have investigated the effect of HPWVA on the current collapse characteristics of AlGaIn/GaN HEMTs. It was found that HPWVA prior to SiN passivation, can significantly reduce device dynamic R<sub>on</sub>, thereby, demonstrating current collapse mitigation by HPWVA. XPS investigations suggest oxygen incorporation, which may eventually lead to the formation of an oxide layer suitable for passivation and filling up of near-surface nitrogen vacancies. On the basis of this account, we believe that HPWVA is a highly feasible and promising alternative for achieving high performance in AlGaIn/GaN HEMTs designed for power switching applications.

## ACKNOWLEDGEMENTS

The authors would like to thank Prof. Tamotsu Hashizume and Dr. Zenji Yatabe of Hokkaido University for their highly valuable assistance during the XPS measurements.

## REFERENCES

- [1] U. K. Mishra, et al., Proc. IEEE **90**, 1022 (2002).
- [2] R. Vetury, et al., IEEE Trans. Electron Devices **48**, 560 (2001).
- [3] D. J. Meyer et al., CS MANTECH Technical Digest, pp. 305-307, April 2008.
- [4] Y. Sakaida et al., CS MANTECH Technical Digest, pp. 197-200, May 2008.
- [5] K. Yoshitsugu, et al., IEICE Tech. Rep. **113**, 7 (2013).
- [6] M. T Hasan et al., IEEE EDL **34**, 1379 (2014).
- [7] J. Joh et al., IEEE TED **58**, 132 (2011).
- [8] W. Shockley et al., Phys. Rev. **87**, 835 (1952).
- [9] N. Shiozaki et al., J. Appl. Phys. **105**, 064912 (2009).
- [10] J. F. Moulder, et al., Handbook of X-ray Photoelectron Spectroscopy, Minnesota: Perkin-Elmer, 1993, p. 14.
- [11] T. Kawanago, et al., IEEE Trans. Electron Devices **61**, 785 (2014).
- [12] T. Hashizume, J. Appl. Phys. **94**, 434 (2003).
- [13] D. P. Butt, et al., J. Nucl. Mater. **264**, 71 (1999).
- [14] T. Akatsu, et al., J. Appl. Phys. **86**, 7146 (1999).
- [15] P. Panchaipetch, et al., Jpn. J. Appl. Phys. **45**, L120 (2006).
- [16] M. J. Hale, et al., J. Chem. Phys. **119**, 6719 (2003).
- [17] C. L. Hinkle, et al., ECS Trans. **19**, 387 (2009).
- [18] D. L. Winn, et al., J. Chem. Phys. **127**, 134705 (2007).
- [19] C. L. Hinkle, et al., Appl. Phys. Lett. **94**, 162101 (2009).
- [20] B. Brennan, et al., Appl. Phys. Lett. **101**, 211604 (2012).

## ACRONYMS

- HEMT: high-electron-mobility transistor
- NDR: normalized dynamic R<sub>on</sub>
- HPWVA: high pressure water vapor annealing
- XPS: x-ray photoelectron spectroscopy